This is an open access article published under a Creative Commons Attribution (CC-BY) License, which permits unrestricted use, distribution and reproduction in any medium, provided the author and source are cited.

ACS AuthorChoice

NANO LETTERS

Letter

pubs.acs.org/NanoLett

Toward Two-Dimensional All-Carbon Heterostructures via Ion Beam Patterning of Single-Layer Graphene

Jani Kotakoski,[*,†] Christian Brand,[‡] Yigal Lilach,[§] Ori Cheshnovsky,[§,∥] Clemens Mangler,[†] Markus Arndt,[‡] and Jannik C. Meyer[†]

[†]Faculty of Physics, PNM and [‡]Faculty of Physics, VCQ, QuNaBioS, University of Vienna, Boltzmanngasse 5, A-1090 Vienna, Austria

[§]The Center for Nanosciences and Nanotechnology and [∥]School of Chemistry, The Raymond and Beverly Faculty of Exact Sciences, Tel Aviv University, Tel Aviv 69978, Israel

ABSTRACT: Graphene has many claims to fame: it is the thinnest possible membrane, it has unique electronic and excellent mechanical properties, and it provides the perfect model structure for studying materials science at the atomic level. However, for many practical studies and applications the ordered hexagon arrangement of carbon atoms in graphene is not directly suitable. Here, we show that the atoms can be locally either removed or rearranged into a random pattern of polygons using a focused ion beam (FIB). The atomic structure of the disordered regions is confirmed with atomic-resolution scanning transmission electron microscopy images. These structural modifications can be made on macroscopic scales with a spatial resolution determined only by the size of the ion beam. With just one processing step, three types of structures can be defined within a graphene layer: chemically inert graphene, chemically active amorphous 2D carbon, and empty areas. This, along with the changes in properties, gives promise that FIB patterning of graphene will open the way for creating all-carbon heterostructures to be used in fields ranging from nanoelectronics and chemical sensing to composite materials.

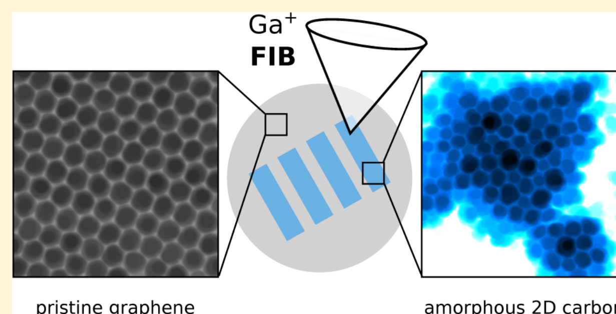

KEYWORDS: *Graphene, focused ion beam, amorphization, scanning transmission electron microscopy*

Graphene has received enormous attention since its introduction a decade ago.[1] Because of its two-dimensional (2D) nature, all atoms in graphene are directly exposed to external interactions through electric and magnetic fields or via chemical and physical processes. This provides a great opportunity for engineering its properties. It is well understood[2] that a controlled rearrangement of the atoms in graphene from the honeycomb pattern into other structures will affect the electronic properties of the material (for example, by introducing a band gap due to scattering of charge carriers[3]) and increase its chemical reactivity.[4] Also, nanocrystalline graphene manufactured from self-assembled molecular monolayers has been shown to be insulating[5] indicating the wide range of electronic properties accessible via manipulation of graphene. However, the considerable challenge of manipulating the atomic structure of a 2D object has so far limited the number of studies on this topic.

Perhaps the most versatile method for the manipulation of materials today is ion irradiation. Its application on the nanoscale, however, requires developing a detailed atomic level understanding on irradiation effects. This is because methods for estimating ion irradiation effects in bulk materials can rarely be directly used for low-dimensional structures,[6] and the optimal irradiation parameters change drastically from bulk to nanomaterials. For example, ion implantation of graphene only becomes possible when the energies are reduced to less than 100 eV,[7−9] which is orders of magnitude lower than in a typical implantation process.

Until now, only rarely has any atomic-level information been obtained for ion irradiation of 2D materials, either through atomistic simulations[6,7,10,11,13−15] or via direct atomic-scale imaging of resulting point defects.[9,16−20] Instead, many studies have used nonlocal methods such as Raman spectroscopy to analyze the disorder.[21−28] Also, in most studies the irradiated structure was the interface between graphene and a substrate rather than suspended graphene. In this case, the underlying material always contributes to the observed changes.[13−15] So far, on SiO_2 substrate, a transition from pristine graphene through a nanocrystallite structure into an amorphous material has been indirectly observed following Ga^+ ion irradiation at 30 keV.[22] This is similar to what has been found during 100 keV electron irradiation of suspended graphene.[29,30] Also the effect of swift heavy ion irradiation at grazing angles has been studied with graphene on a substrate.[31,32] A recent study explored defects created via irradiation of suspended graphene with 30 keV He^+ ions. At an angle of 30°, which was used in the study, such irradiation has been predicted to produce almost exclusively single vacancies.[10] Correspondingly, even at a

Received: May 26, 2015
Revised: July 6, 2015
Published: July 10, 2015

 © 2015 American Chemical Society

DOI: 10.1021/acs.nanolett.5b02063
Nano Lett. 2015, 15, 5944−5949

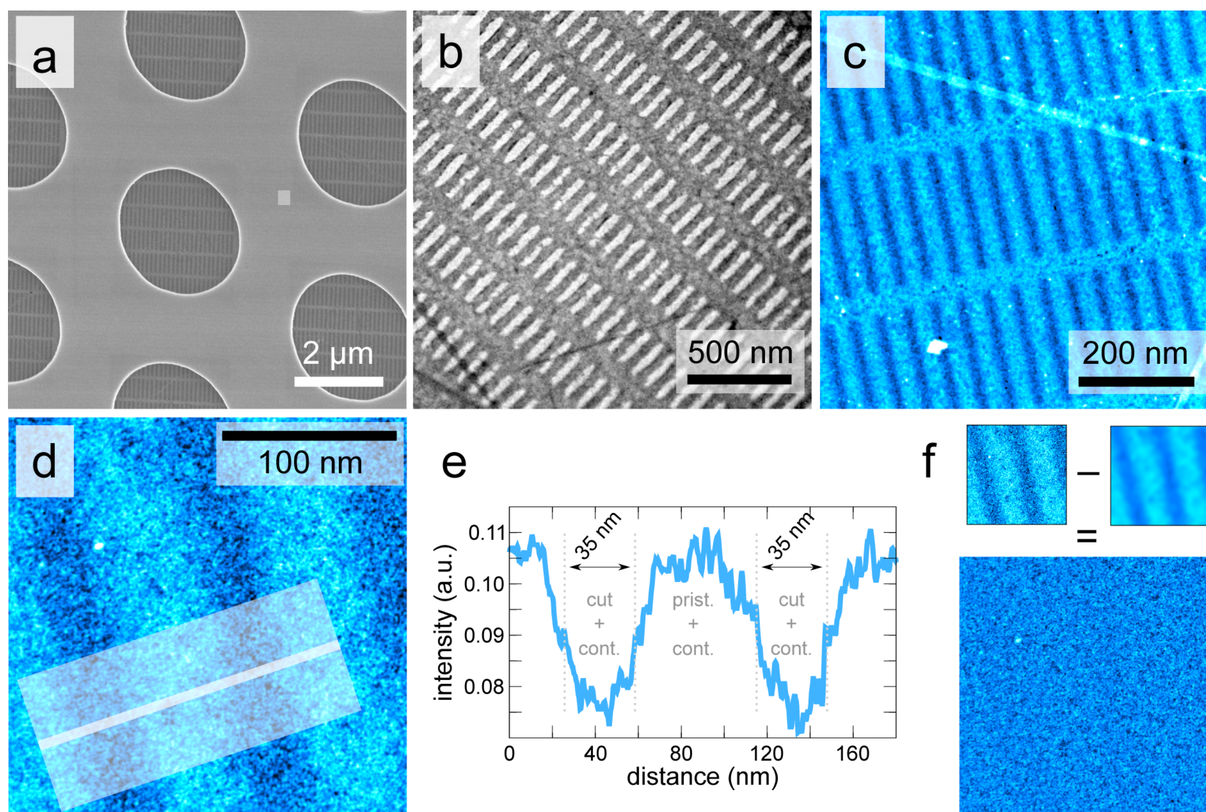

Figure 1. Overview images of the structures patterned into graphene with a focused ion beam. (a) SEM overview image of the SiN_x TEM grid showing an array of holes with a diameter of 2.5 μm. Graphene covers the complete area and is suspended over the holes. The pattern written with the FIB at a dose of 4.96 pC/nm^2 is visible as dark stripes on the suspended membranes. (b) TEM image of a pattern written at a dose of 15.2 pC/nm^2. The white areas correspond to completely removed graphene. (c) STEM-MAADF image of a low-dose pattern (darker areas correspond to lower amount of matter). (d) Higher-magnification STEM-MAADF image of structures written with the lower dose. (e) Line profile from the area marked in panel (d) showing the width of the patterns to be approximately 35 nm. (f) Same image as in panel (d) with the effect of the FIB patterning hidden by subtracting a blurred image (Gaussian blur with radius of 20 px). The resulting image shows only the features of the hydrocarbon contamination on the sample.

fluence of ~10^{16} ions/cm^2, mostly individual point defects were observed.

Here, we show that perpendicular irradiation with a focused beam of Ga^+ ions at 35 keV results in amorphization of suspended graphene at a dose of about 3.1×10^{15} ions/cm^2. Doses three times as high lead to perforation of the membrane, allowing its use, for example, as the thinnest possible beam splitter for matter-wave interferometry.[33] As shown via atomic-resolution scanning transmission electron microscopy (STEM) medium angle angular dark field (MAADF) images, the amorphous areas remain two-dimensional and consist of a variety of carbon rings with sizes ranging from five to nine atoms (with occasional pores) and are similar to the amorphous 2D carbon structure created with electron irradiation of graphene.[29,30] In contrast to transmission electron microscopy (TEM), focused ion beam (FIB) processing can be easily done for areas encompassing square millimeters. With the parameters used in this study, it allows writing pores and amorphized areas into graphene with spatial accuracy down to 35 nm.

The patterns were written into single-layer graphene that was grown via chemical vapor deposition and suspended on a holey SiN_x substrate, using a focused beam of Ga^+ ions with an energy of 35 keV. The substrate contains an array of circular holes that each have a diameter of about 2.5 μm, over which the graphene is suspended. Figure 1a shows an overview scanning electron microscopy (SEM) image of one pattern. A higher magnification TEM image of a pattern written on another sample with a higher dose of Ga^+ is shown in Figure 1b. While the low-dose irradiation has not perforated the graphene, the higher dose has resulted in an array of holes.

To study the structure of the patterned areas at a smaller scale, we used STEM-MAADF imaging with the Nion UltraSTEM 100[34] microscope at 60 kV. The combination of the low acceleration voltage and ultrahigh vacuum (10^{-9} mbar at the sample) ensures that no beam-induced damage will occur even at the irradiated areas, although the kinetic energy of the imaging electrons still suffices to rotate bonds at defects in graphene.[20,35] An overview STEM-MAADF image of a pattern written with the lower dose is shown in Figure 1c. The image in Figure 1d shows a closer view of another low-dose region, which allows measuring the width of the written structures (Figure 1e) to be about 35 nm. This corresponds to the estimated beam size of 20−30 nm of the FIB. The same image also shows that the hydrocarbon contamination on top of graphene is continuous over the pattern and has a similar appearance everywhere. This can be seen in Figure 1f, where a blurred version of the image is subtracted from the original image to bring out the contamination pattern, which at this length scale looks like noise. However, the small dark areas actually correspond to areas where noncontaminated parts of the sample were found.

DOI: 10.1021/acs.nanolett.5b02063
Nano Lett. 2015, 15, 5944−5949

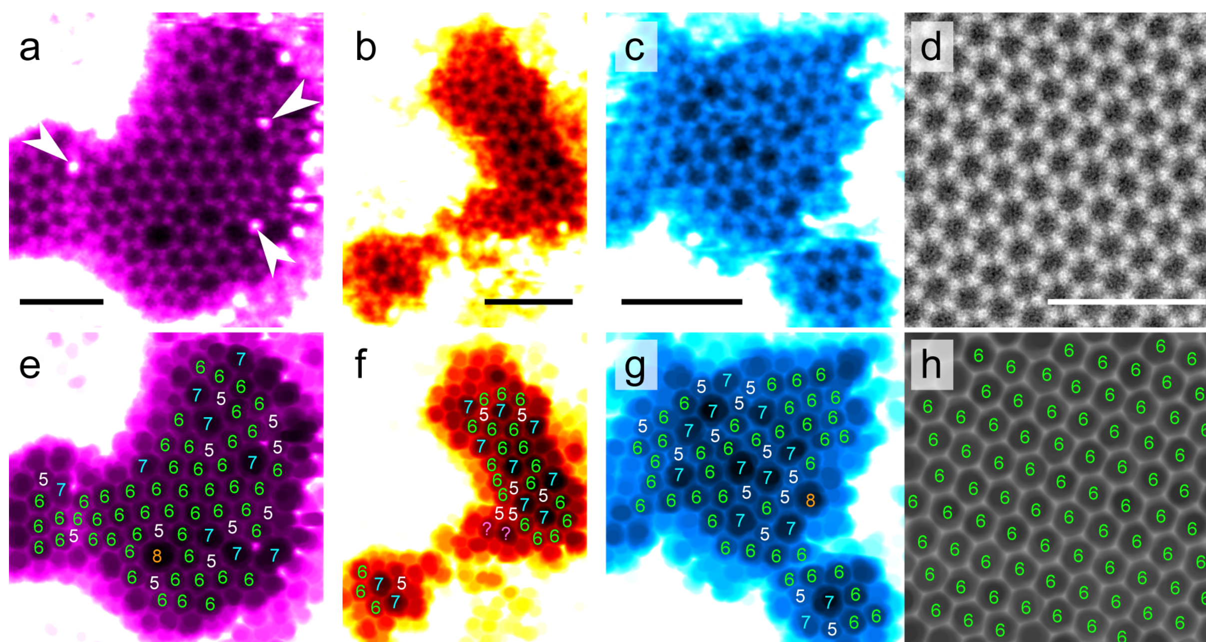

Figure 2. Atomic-resolution images of amorphized graphene areas. (a−d) Example STEM-MAADF images from the amorphized areas (a−c) and a pristine area (d). A deconvolution with the beam profile, modeled as a sum of two Gaussians, has been applied as described in ref 36, followed by a Gaussian blur for panels (a−c) with a radius of 2−3 pixels. (e−h) Same images after the application of a minimum filter with a radius of 10 pixels to enhance the visibility of the nonhexagonal rings with the size of each ring marked on top of the rings. The marked atoms in panel (a) were identified as Si based on the contrast in the MAADF images. The bright areas around the atomically thin structures are covered by hydrocarbon contamination. All scale bars are 1 nm. Each pair of images is colored uniquely to ease the comparison.

Contamination is one of the hardest challenges in working with suspended graphene membranes. In our case, the situation is further worsened by the additional deposition of contamination that occurs during SEM imaging. However, a small fraction of the sample surface remained clean enough to image the atomic structure. Atomic resolution images of the irradiated but not perforated areas are shown in Figure 2a−c and pristine graphene in the nonpatterned part of the same hole in Figure 2d. In every clean area of the irradiated graphene, we found nonhexagonal carbon rings indicating irradiation-induced structural changes with occasional Si atoms incorporated into the nonhexagonal rings (see Figure 2a). Analysis of all of the imaged amorphized areas resulted in the following fractions for the different ring sizes: (5) 22.5%, (6) 63.2%, (7) 13.1%, (8) 0.9%, and (9) 0.4% (in total 818 rings were identified from the images). As in ref 30, we define the crystallinity as the number of hexagons divided by the total number of rings. In the present irradiated material, a crystallinity of 63% is found, while in ref 30 it was 51%. Hence, the amorphization here is close but not quite as strong as in ref 30 although the material is already a random network structure with no nanometer-scale crystalline areas.

A rough estimation for the number of carbon atoms removed from the amorphized areas during ion irradiation can be obtained from the ratios of average intensities (irradiated versus nonirradiated area) in annular dark field images (with background subtracted). This yields a ratio of 91%, which indicates that the amorphized areas have approximately 9% density deficit as compared to pristine graphene. Comparing this number with earlier estimations of electron irradiation-amorphization of graphene[30] shows that such deficit is close to the completely disordered material, as is consistent with our atomic-resolution images. It is also an almost exact match with the density deficit at which the electron-beam-amorphized graphene has a crystallinity value of about 63%[30] (the value calculated above for the current material). This serves as an independent validation for the estimated 9% density deficit.

The dose that was sufficient to amorphize graphene was about 4.96 pC/nm^2, which corresponds to $\phi_{am} \approx 31$ ions/nm^2 (or, 3.1×10^{15} ions/cm^2). To put this dose into perspective, it can be compared with the fact that a square nanometer of graphene has about 38.2 atoms. For cutting graphene, a three times higher dose was required ($\phi_{cut} \approx 95$ ions/nm^2, or 9.5×10^{15} ions/cm^2). Ion beam effects for bulk materials are typically estimated based on the concept of stopping power. In the case of 35 keV Ga^+ irradiation of a carbon material, the nuclear stopping power is estimated to be 142 eV/Å and the electronic stopping power 24 eV/Å.[37] For a dose of 31 ions/nm^2, such deposited energy is orders of magnitude more than what is needed to completely disintegrate a single layer of graphene. So, clearly this approach is not directly useful for 2D materials. A better understanding can be reached through a binary collision approximation. Numerical estimate using an empirical repulsive potential[38] leads to a limiting impact parameter of 0.83 Å for a collision that transfers enough kinetic energy from a 35 keV Ga^+ ion to a carbon atom to cause a displacement in graphene (about 23 eV[39]). This is more than half of the bond length in graphene and corresponds to a probability of 83% for an ion to displace at least one of the target atoms, taking into account the area each carbon atom occupies in the graphene lattice.

Atomistic simulations[6] predict that under our experimental conditions defects will be created with a ratio of approximately 1:1:2 for single vacancies, amorphization events (no atoms sputtered), and complex vacancies (more than one atom sputtered), respectively. The calculated sputtering yield is about 0.55 atoms/ion, which is somewhat lower than what could be expected from the binary collision estimate. This is consistent

DOI: 10.1021/acs.nanolett.5b02063
Nano Lett. 2015, 15, 5944−5949

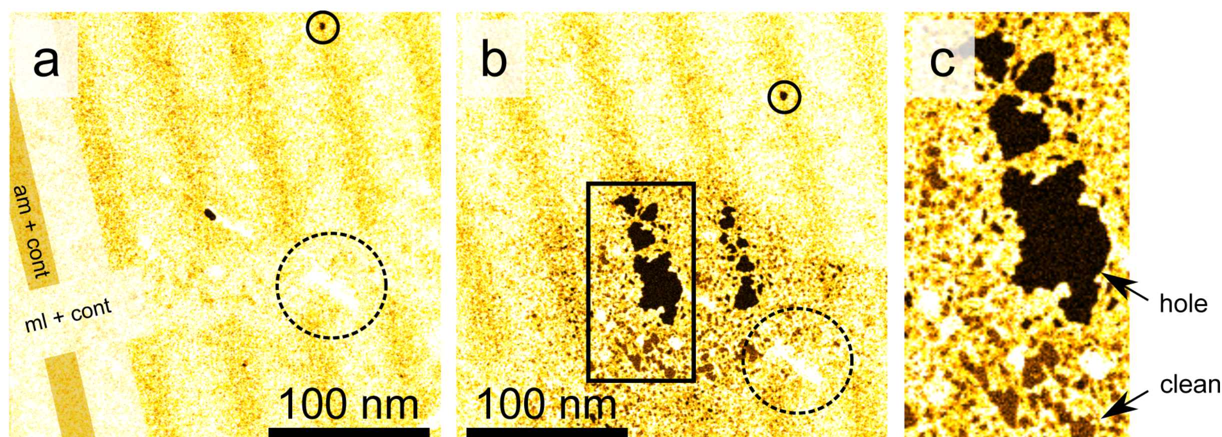

Figure 3. Chemical etching of the amorphous pattern. (a) STEM-MAADF close-up image of a patterned area of the sample before and (b) after an exposure of about 1 h to a parallel electron beam while air was leaked to the objective area of the microscope column (pressure increase from ca. 5.3×10^{-9} to 1.1×10^{-6} mbar). The approximate area exposed to the beam corresponds to the darkened circular shape seen in panel (b). Partial overlay on the left-hand-side of panel (a) highlights the structure of the pattern ("ml+cont" corresponds to nonirradiated graphene and contamination, whereas "am+cont" refers to amorphized areas). Circles with solid and dashed lines mark the same hole and metal contamination, respectively, in both images to ease the comparison. A higher magnification of the area marked with a rectangle in panel (b) is shown in panel (c) to ease distinguishing holes and clean graphene from each other.

with the assumption that for perpendicular irradiation the atoms are typically scattered in the plane and not necessarily removed from it. For a more accurate estimate of the number of sputtered atoms, we need to take into account the increasing vacancy concentration in the structure during irradiation,[11] which leads to an approximation formula for low vacancy concentrations[12]

$$c_v(\phi) = \frac{1}{\frac{n}{(\phi Y_0)} + \gamma} \tag{1}$$

where ϕ is the irradiation dose (ions/nm^2), $n \approx 38.2$ atoms/nm^2 the density of graphene, $Y_0 \approx 0.55$ sputtering yield at $c_v = 0$ and γ a constant that can be obtained through simulations.[11] On the basis of data for Ar^+ and Xe^+ irradiation at 30 keV, γ can be expected to be between 0.5 and 0.8 for Ga^+ irradiation of graphene at 35 keV. For $\gamma = 0.65$, we get $c_v(\phi_{am}) \approx 35\%$ and $c_v(\phi_{cut}) > 70\%$. In contrast to 35% density deficit in the amorphized structure, the two independent estimates described above yielded a value of 9%. This discrepancy is most likely caused by the increased chemical reactivity of vacancies that attract carbon (and occasionally silicon) atoms from the contamination.

The ultrahigh vacuum column of the microscope reduces chemical etching to practically zero, simplifying the analysis of dynamical processes. However, at the same time all beneficial chemical reactions due to water (and other) molecules cracked by the imaging electrons, which could reduce the hydrocarbon contamination, are also prevented. To test both how the contamination is bound to the graphene and how amorphization affects the chemical inertness of graphene, we let air into the microscope column after initial imaging by opening a leak valve. We exposed the structure to a parallel electron beam while increasing the pressure in the objective from 5.3×10^{-9} to 1.1×10^{-6} mbar over an hour. The results of this treatment are shown in Figure 3. The contamination decreased dramatically and several clean areas appeared in the non-irradiated area of the sample, whereas holes grew in the irradiated areas. This demonstrates that controlled amorphization of graphene will activate it chemically. Because we were able to clean parts of the contamination, it cannot be covalently bound to the sample. Therefore, one possible way to overcome the contamination problem could be high-temperature vacuum annealing, which can be expected to remove most of the floating hydrocarbons.

As a conclusion, we have shown that the regular hexagon pattern of single-layer graphene can be selectively either sputtered or transformed into a random pattern of polygons ranging from pentagons to octagons and nine-membered carbon rings in a controlled manner using a focused Ga^+ ion beam at 35 keV. This allows defining three different kinds of areas into a graphene layer with just one processing step with the FIB: chemically inert highly conductive graphene, chemically active, presumably less conductive, amorphous 2D carbon, and empty holes. The smallest demonstrated feature size was about 35 nm. A dose of $\phi_{am} \approx 30$ ions/nm^2 was found to nearly completely amorphize graphene, whereas $\phi_{cut} \approx 100$ ions/nm^2 leads to its perforation. The amorphous areas showed a density deficit of about 9% in discrepancy with an expected value of about 35%. This discrepancy is likely due to filling of the vacancies from the hydrocarbon contamination covering the graphene sheet. This point is supported by the observation of Si atoms immersed into the defected structures. The amorphized regions have a crystallinity value of 63%. The chemical activation gives promise to the application of selectively amorphized graphene in fields ranging from chemical sensing[4] to functionalized membranes and composite materials, while the predicted introduction of a band gap[3] allows their utilization in all-carbon electronics.

Methods. *Samples.* We used commercial single-layer graphene samples (Ted Pella Inc., Redding/CA 21712-5 PELCO) grown with chemical vapor deposition and deposited on SiN_x transmission electron microscopy grids with a regular pattern of holes with an approximate diameter of 2.5 μm.

Focused Ion Beam. Fully and partially sputtered areas were written on different single-layer graphene samples using a focused beam of 35 keV Ga^+ ions (Raith Ionline FIB). The beam size was approximately 20−30 nm, and the writing was performed in a linelike fashion with a step size of 1 nm and a dwell time of 0.0179 ms for the partially sputtered areas, which

DOI: 10.1021/acs.nanolett.5b02063
Nano Lett. 2015, 15, 5944−5949

were later confirmed to be amorphized. The corresponding line dose was 1240 pC/cm. For fully sputtered areas, the dose was 3800 pC/cm (dwell time of 0.0482 ms). For the sample with the lower dose, a pattern of 27 × 6 slits, each 500 nm long, and separated 100 nm from each other, was designed to completely cover the 2.5 μm substrate holes in an area fully covered by graphene. This pattern was duplicated with the same hexagonal periodicity as the circular holes. The whole pattern was milled into the holes by taking a FIB image of a 30 × 30 μm^2 area covered with graphene (with as short as possible exposure to the beam to avoid additional damage to the graphene) and fitting the pattern onto the holes. Milling such a pattern takes about 1 min.

Electron Microscopy. The SEM image in Figure 1a was recorded with Jeol 6700F SEM and the TEM image in Figure 1b with a table top Delong Instruments LVEM5 microscope. High-resolution imaging was carried out with a Nion UltraSTEM 100. The device is equipped with a cold field emission gun, which was operated at 60 kV in ultrahigh vacuum (5.3×10^{-9} mbar at the sample). A medium angle annular dark-field detector was used to record the images. At the end of the experiment, we let air into the microscope column under a parallel electron beam to partially remove the contamination and to test the chemical reactivity. The pressure was increased over a period of an hour to 1.1×10^{-6} mbar. In nonirradiated areas, this procedure uncovered pristine graphene. In the amorphized parts, the chemical processes lead additionally to the appearance of pores.

■ AUTHOR INFORMATION

Corresponding Author

*E-mail: jani.kotakoski@iki.fi.

Notes

The authors declare no competing financial interest.

■ ACKNOWLEDGMENTS

We acknowledge funding from the Austrian Science Fund (FWF) projects M 1481-N20 and P 25721-N20, Wiener Wissenschafts-, Forschungs- und Technologiefonds (WWTF) project MA14-009, European Research Council (ERC) Projects No. 336453-PICOMAT and No. 320694, and European Union Commission Project No. 304886-NANOQUESTFIT. C.B. acknowledges financial support by the Alexander von Humboldt foundation.

■ REFERENCES

(1) Novoselov, K. S.; Jiang, D.; Schedin, F.; Booth, T. J.; Khotkevich, V. V.; Morozov, S. V.; Geim, A. K. Two-dimensional atomic crystals. *Proc. Natl. Acad. Sci. U. S. A.* **2005**, *102*, 10451−10453.

(2) Geim, A. K. Graphene: status and prospects. *Science* **2009**, *324*, 1530−1534.

(3) Lherbier, A.; Roche, S.; Restrepo, O. A.; Niquet, Y.-M.; Delcorte, A.; Charlier, J.-C. Highly defective graphene: A key prototype of two-dimensional Anderson insulators. *Nano Res.* **2013**, *6*, 326−334.

(4) Salehi-Khojin, A.; Estrada, D.; Lin, K. Y.; Bae, M.-H.; Xiong, F.; Pop, E.; Masel, R. I. Polycrystalline Graphene Ribbons as Chemiresistors. *Adv. Mater.* **2012**, *24*, 53−57.

(5) Turchanin, A.; et al. Conversion of Self-Assembled Monolayers into Nanocrystalline Graphene: Structure and Electric Transport. *ACS Nano* **2011**, *5*, 3896−3904.

(6) Lehtinen, O.; Kotakoski, J.; Krasheninnikov, A. V.; Tolvanen, A.; Nordlund, K.; Keinonen, J. Effects of ion bombardment on a two-dimensional target: Atomistic simulations of graphene irradiation. *Phys. Rev. B: Condens. Matter Mater. Phys.* **2010**, *81*, 153401.

(7) Åhlgren, E.; Kotakoski, J.; Krasheninnikov, A. Atomistic simulations of the implantation of low-energy boron and nitrogen ions into graphene. *Phys. Rev. B: Condens. Matter Mater. Phys.* **2011**, *83*, 115424.

(8) Xu, Y.; Zhang, K.; Brüsewitz, C.; Wu, X.; Hofsäss, H. C. Investigation of the effect of low energy ion beam irradiation on mono-layer graphene. *AIP Adv.* **2013**, *3*, 072120.

(9) Bangert, U.; et al. Ion implantation of graphene - towards IC compatible technologies. *Nano Lett.* **2013**, *13*, 4902−4907.

(10) Lehtinen, O.; Kotakoski, J.; Krasheninnikov, A. V.; Keinonen, J. Cutting and controlled modification of graphene with ion beams. *Nanotechnology* **2011**, *22*, 175306.

(11) Åhlgren, E. H.; Kotakoski, J.; Lehtinen, O.; Krasheninnikov, A. V. Ion irradiation tolerance of graphene as studied by atomistic simulations. *Appl. Phys. Lett.* **2012**, *100*, 233108.

(12) The formula has been established for low c_v and shows asymptotically wrong behaviour for $c_v \to 1$. It can therefore only be trusted for $c_v \ll 1$.

(13) Standop, S.; Lehtinen, O.; Herbig, C.; Lewes-Malandrakis, G.; Craes, F.; Kotakoski, J.; Michely, T.; Krasheninnikov, A. V.; Busse, C. Ion Impacts on Graphene/Ir(111): Interface Channeling, Vacancy Funnels, and a Nanomesh. *Nano Lett.* **2013**, *13*, 1948−1955.

(14) Åhlgren, E. H.; Hämäläinen, S. K.; Lehtinen, O.; Liljeroth, P.; Kotakoski, J. Structural manipulation of the graphene/metal interface with Ar^+ irradiation. *Phys. Rev. B: Condens. Matter Mater. Phys.* **2013**, *88*, 155419.

(15) Herbig, C.; Åhlgren, E. H.; Jolie, W.; Busse, C.; Kotakoski, J.; Krasheninnikov, A. V.; Michely, T. Interfacial Carbon Nanoplatelet Formation by Ion Irradiation of Graphene on Ir(111). *ACS Nano* **2014**, *8*, 12208−12218.

(16) Tapasztó, L.; Dobrik, G.; Nemes-Incze, P.; Vertesy, G.; Lambin, Ph.; Biró, L. P. Tuning the electronic structure of graphene by ion irradiation. *Phys. Rev. B: Condens. Matter Mater. Phys.* **2008**, *78*, 233407.

(17) Ugeda, M. M.; Brihuega, I.; Guinea, F.; Gómez-Rodríguez, J. M. Missing Atom as a Source of Carbon Magnetism. *Phys. Rev. Lett.* **2010**, *104*, 096804.

(18) Ugeda, M. M.; Fernández-Torre, D.; Brihuega, I.; Pou, P.; Martínez-Galera, A. J.; Pérez, R.; Gómez-Rodríguez, J. M. Point defects on graphene on metals. *Phys. Rev. Lett.* **2011**, *107*, 116803.

(19) Ugeda, M. M.; Brihuega, I.; Hiebel, F.; Mallet, P.; Veuillen, J.-Y.; Gómez-Rodríguez, J. M.; Ynduráin, F. Electronic and structural characterization of divacancies in irradiated graphene. *Phys. Rev. B: Condens. Matter Mater. Phys.* **2012**, *85*, 121402.

(20) Pan, C.-T.; Hinks, J. A.; Ramasse, Q. M.; Greaves, G.; Bangert, U.; Donnelly, S. E.; Haigh, S. J. In-situ observation and atomic resolution imaging of the ion irradiation induced amorphisation of graphene. *Sci. Rep.* **2014**, *4*, 6334.

(21) Compagnini, G.; Giannazzo, F.; Sonde, S.; Raineri, V.; Rimini, E. Ion irradiation and defect formation in single layer graphene. *Carbon* **2009**, *47*, 3201−3207.

(22) Zhou, Y.-B.; Liao, Z.-M.; Wang, Y.-F.; Duesberg, G. S.; Xu, J.; Fu, Q.; Wu, X.-S.; Yu, D.-P. Ion irradiation induced structural and electrical transition in graphene. *J. Chem. Phys.* **2010**, *133*, 234703.

(23) Compagnini, G.; Forte, G.; Giannazzo, F.; Raineri, V.; La Magna, A.; Deretzis, I. Ion beam induced defects in graphene: Raman spectroscopy and DFT calculations. *J. Mol. Struct.* **2011**, *993*, 506−509.

(24) Kalbac, M.; Lehtinen, O.; Krasheninnikov, A. V.; Keinonen, J. Ion-Irradiation-Induced Defects in Isotopically-Labeled Two Layered Graphene: Enhanced In-Situ Annealing of the Damage. *Adv. Mater.* **2013**, *25*, 1004−1009.

(25) Wang, Q.; Mao, W.; Ge, D.; Zhang, Y.; Shao, Y.; Ren, N. Effects of Ga ion-beam irradiation on monolayer graphene. *Appl. Phys. Lett.* **2013**, *103*, 073501.

(26) Zeng, J.; Yao, H. J.; Zhang, S. X.; Zhai, P. F.; Duan, J. L.; Sun, Y. M.; Li, G. P.; Liu, J. Swift heavy ions induced irradiation effects in monolayer graphene and highly oriented pyrolytic graphite. *Nucl. Instrum. Methods Phys. Res., Sect. B* **2014**, *330*, 18−23.

DOI: 10.1021/acs.nanolett.5b02063
Nano Lett. 2015, 15, 5944−5949

(27) Mathew, S.; et al. Mega-electron-volt proton irradiation on supported and suspended graphene: A Raman spectroscopic layer dependent study. *J. Appl. Phys.* **2011**, *110*, 084309.
(28) Kumar, S.; Tripathi, A.; Khan, S. A.; Pannu, C.; Avasthi, D. K. Radiation stability of graphene under extreme conditions. *Appl. Phys. Lett.* **2014**, *105*, 133107.
(29) Kotakoski, J.; Krasheninnikov, A. V.; Kaiser, U.; Meyer, J. C. From Point Defects in Graphene to Two-Dimensional Amorphous Carbon. *Phys. Rev. Lett.* **2011**, *106*, 105505.
(30) Eder, F. R.; Kotakoski, J.; Kaiser, U.; Meyer, J. C. A journey from order to disorder Atom by atom transformation from graphene to a 2d carbon glass. *Sci. Rep.* **2014**, *4*, 4060.
(31) Ochedowski, O.; Akcöltekin, S.; Ban d'Etat, B.; Lebius, H.; Schleberger, M. Detecting swift heavy ion irradiation effects with graphene. *Nucl. Instrum. Methods Phys. Res., Sect. B* **2013**, *314*, 18−20.
(32) Ochedowski, O.; Kleine Bussmann, B.; Ban d'Etat, B.; Lebius, H.; Schleberger, M. Manipulation of the graphene surface potential by ion irradiation. *Appl. Phys. Lett.* **2013**, *102*, 153103.
(33) Brand, C.; Sclafani, M.; Knobloch, C.; Lilach, Y.; Juffmann, T.; Kotakoski, J.; Mangler, C.; Winter, A.; Turchanin, A.; Meyer, J. C.; Cheshnovsky, O.; Arndt, M. An atomically thin matter-wave beam splitter *Nature Nanotech.* in press, **2015**.
(34) Krivanek, O. L.; Corbin, G. J.; Dellby, N.; Elston, B. F.; Keyse, R. J.; Murfitt, M. F.; Own, C. S.; Szilagyi, Z. S.; Woodruff, J. W. An electron microscope for the aberration-corrected era. *Ultramicroscopy* **2008**, *108*, 179−195.
(35) Kotakoski, J.; Mangler, C.; Meyer, J. C. Imaging atomic-level random walk of a point defect in graphene. *Nat. Commun.* **2014**, *5*, 4991.
(36) Krivanek, O. L.; et al. Atom-by-atom structural and chemical analysis by annular dark-field electron microscopy. *Nature* **2010**, *464*, 571−574.
(37) Calculated with the approach introduced in ref 38 and implemented in the code TRIM.
(38) Ziegler, J. F.; Biersack, J. P.; Littmark, U. *The Stopping and Range of Ions in Solids*; Pergamon: New York, 1985.
(39) Meyer, J. C.; et al. Accurate Measurement of Electron Beam Induced Displacement Cross Sections for Single-Layer Graphene. *Phys. Rev. Lett.* **2012**, *108*, 196102.

DOI: 10.1021/acs.nanolett.5b02063
Nano Lett. 2015, 15, 5944−5949